energies

MDPI

Article

Impact of Ambient Temperature on the Performance of Liquid Air Energy Storage Installation

Aleksandra Dzido * and Piotr Krawczyk

Institute of Heat Engineering, Warsaw University of Technology, Nowowiejska 21/25, 00-665 Warsaw, Poland; piotr.krawczyk@pw.edu.pl
* Correspondence: aleksandra.dzido@pw.edu.pl

Abstract

The increasing share of renewable energy sources (RES) in modern power systems necessitates the development of efficient, large-scale energy storage technologies capable of mitigating generation variability. Liquid Air Energy Storage (LAES), particularly in its adiabatic form, has emerged as a promising candidate by leveraging thermal energy storage and high-pressure air liquefaction and regasification processes. Although LAES has been widely studied, the impact of ambient temperature on its performance remains insufficiently explored. This study addresses that gap by examining the thermodynamic response of an adiabatic LAES system under varying ambient air temperatures, ranging from 0 °C to 35 °C. A detailed mathematical model was developed and implemented in Aspen Hysys to simulate the system, incorporating dual refrigeration loops (methanol and propane), thermal oil intercooling, and multi-stage compression/expansion. Simulations were conducted for a reference charging power of 42.4 MW at 15 °C. The influence of external temperature was evaluated on key parameters including mass flow rate, unit energy consumption during liquefaction, energy recovery during expansion, and round-trip efficiency. Results indicate that ambient temperature has a marginal effect on overall LAES performance. Round-trip efficiency varied by only ±0.1% across the temperature spectrum, remaining around 58.3%. Mass flow rates and power output varied slightly, with changes in discharging power attributed to temperature-driven improvements in expansion process efficiency. These findings suggest that LAES installations can operate reliably across diverse climate zones with negligible performance loss, reinforcing their suitability for global deployment in grid-scale energy storage applications.

Keywords: liquid air energy storage; mathematical modelling; energy storage; aspen hysys; adiabatic LAES

Check for updates

Academic Editors: Ahmed Chiheb Ammari and Ahmed S. A. Awad

Received: 26 October 2025
Revised: 15 December 2025
Accepted: 19 December 2025
Published: 28 December 2025

Copyright: © 2025 by the authors. Licensee MDPI, Basel, Switzerland. This article is an open access article distributed under the terms and conditions of the Creative Commons Attribution (CC BY) license.

1. Introduction

The global demand for electricity continues to rise due to population growth, industrialization, and the increasing use of electronic devices. Global primary energy consumption reached 183,230 TWh in 2023 [1]. As a result, the development of renewable energy sources (RES) has become a priority in many regions. In tropical climates, solar power is widely utilized due to high solar radiation throughout the year. In temperate zones, a combination of solar and wind energy is common [2], as seasonal variations provide opportunities for both. Meanwhile, in polar and mountainous regions, hydropower and wind energy are key solutions, leveraging strong winds and abundant water resources [3]. The transition to

renewable energy is essential to meet growing electricity needs while reducing dependence on fossil fuels and minimizing environmental impact.

Some of these RES like solar and wind powers are weather-dependent sources [4]. Their operation in significant share in the national power systems causes serious challenges like mismatch between supply and demand, need to adjust the electricity grid, and renewables' cooperation with more stable sources like nuclear power plants or fossil fuel plants, which cannot change the load rapidly [5].

One of the solutions for these problems is the development of high-efficiency, long-term and high-capacity energy storage installations [6]. Typical technologies for system-scale electricity storage are pumped hydro (PH) [7] and Compressed Air Energy Storage (CAES) [8]; both have special geological requirements, so cannot be easily applied in every location. Another technology is hydrogen production and reusage, i.e., in fuel cells, which is associated with the main drawback of relatively low efficiency and component long-term performance challenges [9]. Significantly higher efficiency could be obtained in the case of batteries, i.e., flow batteries, but in this case the main drawbacks are short lifetime, significant environmental impact, and economic issues related to the need of materials recycling [10]. Liquid Air Energy Storage (LAES) has emerged as a promising alternative to conventional energy storage technologies [11].

Adiabatic liquid air energy storage (A-LAES) represents an advanced energy storage approach that leverages the inherent thermodynamics of air liquefaction and regasification, where the heat generated during the compression phase is captured, stored, and later reused during expansion to minimize energy losses and improve overall cycle efficiency [12]. In these systems, during the charging cycle, ambient air is compressed and subsequently cooled in multi-stage, intercooled compressors [13]. Then, high-pressure, gaseous air is cooled down to cryogenic temperatures (at the range of −190 °C) and throttled. As a result, the gaseous air partially liquefies. The liquid phase is then stored in a near-ambient-pressure tank. Heat received during compression intercooling is stored in the form of thermal oil (temperature range 200–300 °C) [14]. During the periods of electricity need, the LAES discharging process takes place. Liquid air is pumped to a high pressure (100–150 bar), heated up to re-gasify and superheat, and finally expanded in the turbine sections, typically with intercooling [15], by using thermal oil and a heat source. In such a system optimization of cooling cycles is also crucial. Cold obtained during air regasification in the discharging section can be used in further charging processes to cool air, which contributes to an increase in the round-trip efficiency (RTE) of the storing process.

The thermodynamic framework of adiabatic LAES underscores the careful balance between minimizing irreversibility in compressors and efficient heat transfer during both storage and subsequent reheat stages, with particular emphasis on employing multi-stage compression and expansion units to closely approximate isothermal conditions [8]. Several studies demonstrate that an effective coupling of heat recovery from compression with its reuse in the expansion cycle can lead to notable efficiency enhancements, even overcoming the traditionally low round-trip efficiencies associated with simpler LAES cycles that do not exploit thermal recovery [12]. Recent advancements have focused on optimizing the thermal management system by implementing integrated hot and cold storage strategies, where the recovered compression heat not only assists in the reheat process but also reduces the network requirement during liquefaction by recycling available thermal energy [16]. Moreover, hybrid LAES configurations have emerged that combine the benefits of adiabatic heat recovery with additional thermodynamic cycles, such as Organic Rankine or Brayton cycles, further enhancing the system's round-trip efficiency and operational flexibility for large-scale, grid-level applications [8].

The development of high-performance heat exchangers and regenerator designs plays a critical role in these systems, where multi-stream heat exchangers enable effective temperature matching between working fluids while reducing entropy generation, thus optimizing the thermal integration between the compression and expansion phases [17]. Furthermore, thermo-economic analyses indicate that while capital costs related to advanced heat recovery components can be high, the improvement in energy efficiency and the resulting higher round-trip efficiency potentially reduce the levelized cost of storage [18].

Experimental and simulation-based research projects have validated these concepts by demonstrating that adiabatic LAES systems with robust heat recovery measures can achieve round-trip efficiencies in the range of 55–60%, thereby positioning them as strong candidates for intermittent renewable energy integration and grid-balancing applications [19]. Additional research has highlighted the adaptability of adiabatic LAES by coupling it with auxiliary systems that not only allow electric power production but also provide ancillary services such as cooling or heating, which further justifies the investment in advanced TES components [16]. Overall, the literature suggests that the successful integration of compression heat recovery in adiabatic LAES systems is pivotal. This strategy mitigates energy losses that are otherwise inherent in conventional liquefaction and expansion processes, enhances overall system performance, and fosters the economic viability of LAES for large-scale energy storage applications [8].

Ambient temperature variations directly impact the thermodynamic efficiency of liquefaction cycles, as pre-cooled and direct expansion methods depend critically on air temperature differentials [20]. The Linde–Hampson cycle's performance degrades measurably as inlet temperature deviates from design conditions, with dynamic modeling of similar compressed CO_2 systems demonstrating that compressor inlet temperature changes of $\pm$10 K alter system efficiency by 3–5%, while broader temperature perturbations of $\pm$20 K cause power consumption fluctuations of 6–8% [21]. These thermodynamic sensitivities arise because liquefaction efficiency is directly proportional to the available temperature gradient between ambient air and the cryogenic storage temperature; seasonal ambient cycles in temperate climates (ranging $\pm$15 K annually) therefore create predictable but uncharacterized performance degradation pathways. Current LAES literature lacks longitudinal field studies quantifying performance across seasonal temperature ranges, extreme weather events, and comparative installations in diverse climatic regions—a gap that prevents accurate efficiency predictions and prevents the optimization of installation sites for maximum annual performance.

This paper aims to fill this literature gap by analyzing the impact of the ambient temperature on the efficiency and reliability of LAES systems. A better understanding of these effects is essential for optimizing LAES deployment in various climates and improving its feasibility as a large-scale energy storage solution.

2. Methods

The aim of this study was to asses the main LAES parameter of efficiency under various weather conditions. For this purpose, a mathematical model of the main processes occurring in the system was developed. Mathematical modeling serves as a fundamental approach for predicting and optimizing complex chemical engineering processes, enabling systematic analysis of process behavior under varying operational conditions without requiring costly and time-consuming experimental iterations. The mathematical modeling framework integrates several essential methodological components that must be carefully selected and implemented to ensure accurate representation of physical and chemical phenomena.

The mathematical formulation of process models requires the establishment of mass and energy balances coupled with kinetic rate expressions and phase equilibrium rela-

tionships. Differential equations derived from these balances represent the fundamental mathematical description of process dynamics, and their solution requires conversion to systems of difference equations amenable to numerical integration with adaptive spatial or temporal stepping. Our model was based on equilibrium balance equations.

To determine media properties the Peng–Robinson state Equation (1) was used [22]:

$$p = \frac{RT}{v-b} - \frac{a(T)}{v(v+b)+b(v-b)} \tag{1}$$

where: p—pressure [Pa], R—individual ideal gas constant [J/kg·K], T—temperature [K], v—specific volume [m^3/kg], a, b—constants.

The flow through the valves was calculated according to (2) [23].

$$\dot{m} = k\sqrt{\Delta p} \tag{2}$$

$\dot{m}$—mass flow [kg/s], k—coefficient representing the inverse of flow resistance (conductivity) [$\sqrt{\text{kg·m}}$], Δp—pressure drop [Pa].

The mass flow rate depends on the inlet pressure (p_{in}), outlet pressure (p_{out}), and the C_V coefficient corresponding to the inverse of flow resistance (3).

$$\dot{m} = f(p_{in}, p_{out}, C_V) \tag{3}$$

Heat exchangers were modelled as shell-tubes. For the shell side, the energy balance equation takes form of (4)

$$\dot{m}_{shell}\cdot(h_{in} - h_{out})_{shell} - q_{loss} + q = \rho\frac{d(V\cdot h_{out})_{shell}}{dt} \tag{4}$$

where $\dot{m}_{shell}$—mass flow rate at the shell side [kg/s], h_{in}, h_{out}—inlet and outlet enthalpy of the flow [kJ/kg], q_{loss}—heat losses [kW], q—heat provided to the shell side [kW], ρ—density [kg/m^3], t—time [s], V—volume [m^3].

On the other hand, the energy balance equation for the tube side can be expressed as (5)

$$\dot{m}_{tube}\cdot(h_{in} - h_{out})_{tube} - q_{loss} + q = \rho\frac{d(V\cdot h_{out})_{tube}}{dt} \tag{5}$$

where $\dot{m}_{tube}$—mass flow rate at the tube side [kg/s], h_{in}, h_{out}—inlet and outlet enthalpy of the flow [kJ/kg], q_{loss}—heat losses [kW], q—heat provided to the tube side [kW], ρ—density [kg/m^3], t—time [s], V—volume [m^3]

The compressor and expander power were calculated from (6).

$$P = \dot{n}_{in}\cdot M\cdot\left(\frac{n}{n-1}\right)\cdot CF\cdot\left(\frac{p_{in}}{\rho_{in}}\right)\cdot\left[\left(\frac{p_{out}}{p_{in}}\right)^{\left(\frac{n-1}{n}\right)} - 1\right] \tag{6}$$

P—device's power [kW], $\dot{n}_{in}$—inlet molar flow rate [kmol/s], M—molar mass of the working medium [kg/kmol], n—volume exponent, p_{in}, p_{out}—inlet and outlet pressure [Pa], ρ_{in}—inlet density [kg/m^3].

In (6) the correction factor was described as (7).

$$CF = \frac{h'_{out} - h_{in}}{\left(\frac{n-1}{n}\right)\left(\frac{p_{out}}{\rho'_{out}} - \frac{p_{in}}{\rho_{in}}\right)} \tag{7}$$

The power transferred to the working medium during compression was expressed as (8).

$$P = \dot{n}_{in} \cdot M \cdot (h_{out} - h_{in}) \tag{8}$$

Likewise, the expander power, which working medium delivers was calculated according to (9):

$$P = \dot{n}_{in} \cdot M \cdot (h_{in} - h_{out}) \tag{9}$$

In the case of the pump, the ideal power required to increase the medium pressure was given by (10).

$$P = \frac{(p_{out} - p_{in}) \cdot \dot{n}_{in} \cdot M}{\rho} \tag{10}$$

The efficiency of the system was calculated as:

$$\eta = \frac{P_{expander}}{P_{compressor} + P_{pump}} \tag{11}$$

The analyzed system scheme is presented in Figure 1. Note that the LAES installation is equipped with two cooling cycles, due to the high temperature difference. The intercooling process after each compression stage is realized by a thermal oil (n-C20) circuit.

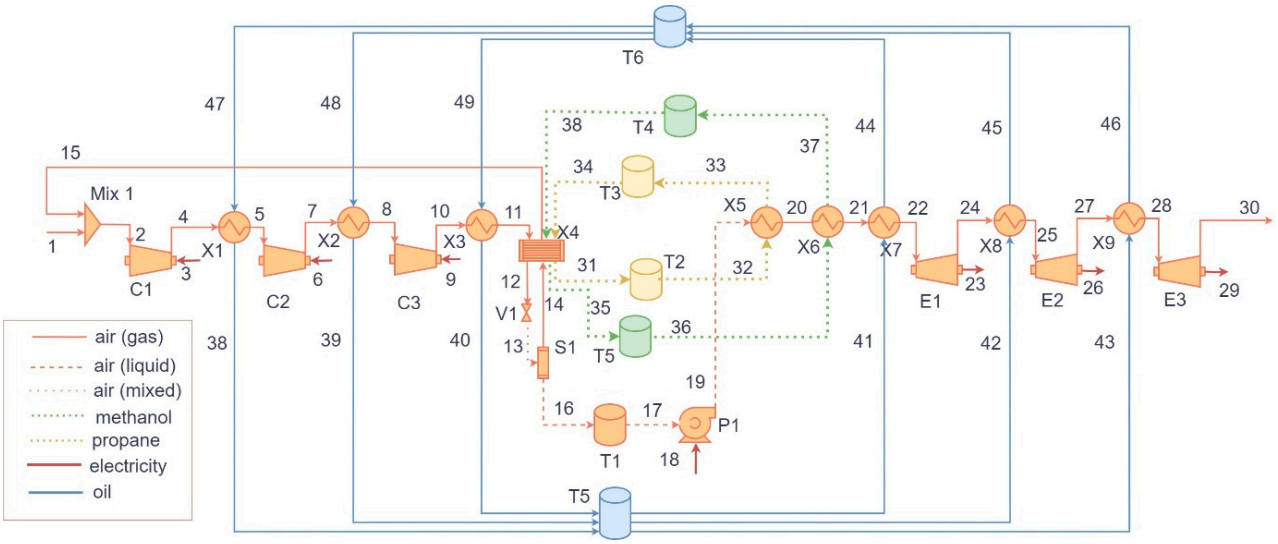


Figure 1. Scheme of the analyzed system. C—compressor, X—heat exchanger, T—insulated tank, P—pump, V—throttling valve, S—phase separator, E—expander, Mix—mixer.

Figure 1 illustrates the schematic configuration of the investigated LAES system. The modelled plant operates according to a charge–discharge cycle and integrates air liquefaction, cryogenic storage, thermal energy storage (TES), and power generation. The system is designed to maximize round-trip efficiency through extensive thermal integration and the use of auxiliary working-fluid loops [24], although phase change materials are also reported as a prospective cold storage dedicated for LAES [25].

During the charging phase, ambient air is drawn into the system and compressed in a multistage compression train (C1–C3). Intercooling between successive compression stages is achieved by air–thermal oil heat exchangers (X1–X3), which reduce the specific compression work. Electrical energy supplied to the compressors represents the primary energy input to the system [10].

The compressed air is subsequently cooled in a cryogenic heat exchanger (X4), where it exchanges heat with cold streams of recirculated air, streams recovered from the discharging

process and cold thermal storage units. As a result, the air temperature is reduced. Then air is being throttled in a Joule–Thomson valve (V1), leading to partial air liquefaction. Low-pressure, gaseous air recirculates via multi-stream heat exchanger (X4), while the liquefied air is then routed to a cryogenic storage tank (T6) for long-term energy storage.

The LAES system incorporates both hot and cold thermal energy storage to enhance overall efficiency. Thermal energy generated during air compression is recovered and stored in a dedicated hot storage tank (T5) in the form of hot thermal oil. This medium is further applied for air pre-heating before expansion during discharging of the store. Conversely, cold energy released during the air expansion and evaporation processes is captured and stored in cold storage tanks (T3 and T4). Two auxiliary cooling loops are involved to provide a liquid operating temperature in a wide range of temperatures, like in [26]. As cooling media, methanol and propane were used [27].

In discharging mode, liquid air is extracted from the cryogenic storage tank and pressurized using a cryogenic pump (P1). The pressurized liquid air is then heated and vaporized through a sequence of heat exchangers (X5–X7), primarily utilizing auxiliary thermal loops and then the stored compression heat (thermal oil).

Following vaporization, the high-pressure air expands through a series of expansion turbines (E1–E3), producing mechanical power that is converted into electricity. The expanded air is finally released to the atmosphere at near-ambient conditions.

3. Model Implementation

The mathematical model described in the previous section was implemented in the Aspen HYSYS® numerical simulation environment. Aspen HYSYS was selected due to its extensive validation and widespread application in the modelling and performance assessment of petrochemical processes, cryogenic systems, and large-scale energy storage technologies [23]. In particular, the software provides robust thermodynamic property packages, steady-state solvers, and heat-integration capabilities that are well suited for the analysis of LAES systems.

Moreover, several studies have successfully applied Aspen HYSYS to the modelling of cryogenic air separation units, liquefaction cycles, and LAES configurations, demonstrating its suitability for such applications [28,29]. Consequently, Aspen HYSYS was considered an appropriate and reliable tool for the present investigation.

The scheme of the implemented system is shown in Figure 2. Air was modelled as a real-gas mixture using the Peng–Robinson equation of state, which is commonly employed for high-pressure and cryogenic air processes. All simulations were conducted under steady-state conditions, with transient effects neglected. Pressure drops in pipelines were assumed to be negligible unless explicitly defined by component pressure ratios.

Heat exchangers were modelled using a fixed minimum temperature approach, ensuring realistic thermal performance and avoiding temperature crossovers. The minimum temperature difference in oil–air heat exchangers was set to $\Delta T = 5\ ^{\circ}C$, consistent with industrial design practices.

The base-case simulations were performed for an ambient temperature of 15 °C, representing typical moderate climatic conditions. Ambient air (assumed as a mixture of nitrogen and oxygen only) was supplied to the compression train with a mass flow rate of 51 $kg \cdot s^{-1}$, which resulted in a total charging power of 42.4 MW.

The air liquefaction section operated at a maximum pressure of 200 bar, while the regasification and expansion section operated at 100 bar. To ensure balanced operation and numerical stability, the pressure ratios of compressors and expanders were equalized across individual stages.

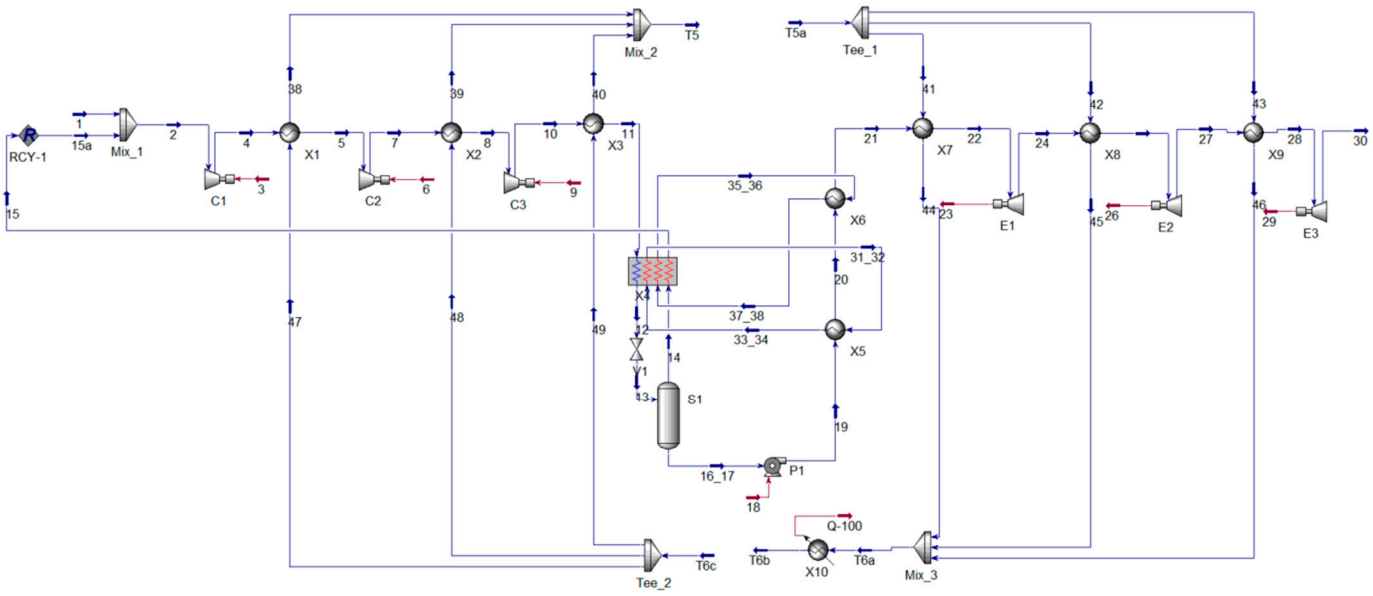


Figure 2. Visualization of the model implementation in Aspen Hysys.

The performance of turbomachinery was represented using constant isentropic efficiencies. The adiabatic efficiency of compressors was assumed to be 82%, while the expanders were assigned a higher efficiency of 90%, reflecting typical performance ranges for industrial-scale equipment. For instance Bhavsar et al. [30] presented a centrifugal air compressor with an efficiency of 84.4%, Li et al. [31] examined a five-stage axial compressor for Compressed Air Energy Storage (CAES), obtaining isentropic efficiencies of 89.3%, and Heidarian et al. [32] showed an axial compressor with efficiency 80.6%. For air expanders an efficiency of 90% was shown in [6,15], 89.94% in [33], and 88.47% in [34].

Liquid-air pressurization was modelled using a cryogenic pump with negligible heat exchange with the environment. Thermal energy storage units were represented as ideal heat reservoirs with fixed inlet and outlet temperatures, allowing effective coupling between the charging and discharging processes.

The charging process involved multistage air compression, intercooling, cryogenic cooling, and liquefaction, followed by storage in a cryogenic tank. The discharging process included liquid-air pumping, regasification using stored thermal energy, and multistage expansion for electricity generation.

The discharging power output was dependent on the charging-to-discharging time ratio (CDTR). For a CDTR value of 2, the calculated discharging power was 49.43 MW, indicating effective power amplification due to thermal energy recovery and liquid-air pumping.

The overall round-trip (storage) efficiency of the LAES system was calculated as 58.3%, defined as the ratio of electrical energy generated during discharge to the electrical energy consumed during charging. This value lies well within the range reported in the literature for advanced LAES systems, exceeding 50% [35], and remaining comparable with values of approximately 50% [36], 48% [14], and 54.16–59.42% [37].

The agreement with previously published results confirms the validity of the modelling approach and parameter selection, and supports the credibility of the developed Aspen HYSYS model for further parametric and optimization studies.

The main thermodynamic parameters of all process streams, including temperatures, pressures, mass flow rates, and phase compositions, are summarized in Table A1 (Appendix A).

4. Results and Analysis

This section presents a parametric analysis of the influence of ambient air temperature on the performance of the LAES system modelled in Aspen HYSYS. As the charging process of LAES is dominated by air compression, the system performance is inherently sensitive to inlet air conditions, particularly temperature. Compressors, as volumetric machines, typically operate at nearly constant volumetric flow rates; therefore, changes in air density due to ambient temperature variations directly affect the inlet mass flow rate, compression work, and overall energy consumption.

In practical applications, LAES installations are expected to operate under variable climatic and site-specific conditions, depending on geographic location and seasonal weather patterns. To account for this variability, the present study investigates ambient air temperatures in the range of 0–35 °C, which represents typical operating conditions encountered in many regions worldwide.

The analysis focuses on the following points:

- Variations in inlet air mass flow rate;
- Unit energy expenditures for air liquefaction and unit energy gains during expansion;
- Round-trip efficiency of the storage system;
- Total charging and discharging power output.

Figure 3 presents the inlet air mass flow rates for the analyzed ambient temperatures. Relative to the base-case condition of 15 °C, the mass flow varies from +5.49% at 0 °C to −6.47% at 35 °C. This trend is a direct consequence of changes in air density with temperature, confirming the expected behavior of volumetric compression systems.

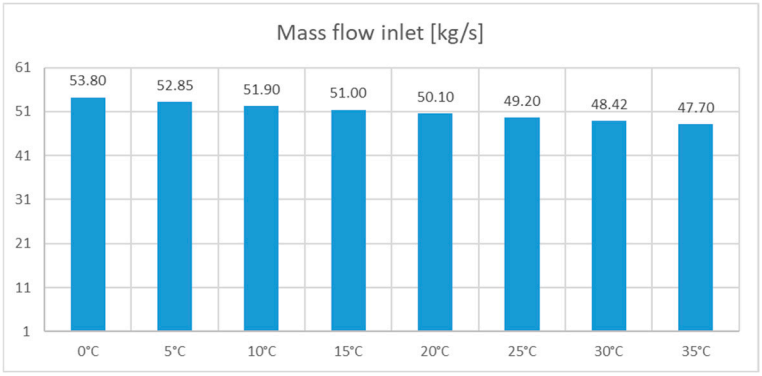


Figure 3. Inlet mass flow for analyzed ambient temperatures.

Despite these variations in mass flow, the unit energy expenditures for air liquefaction remain within a relatively narrow range of 0.219–0.247 kWh·kg^{-1}, as shown in Figure 4. Compared to the reference case at 15 °C, the observed deviations are limited to −5.1% at 0 °C and +6.9% at 35 °C, indicating moderate sensitivity of the liquefaction process to ambient conditions.

Importantly, these values are in good agreement with those reported in the literature for high-pressure LAES and cryogenic air liquefaction systems, which typically range between 0.189–0.295 kWh/kg [38], 0.255 kWh/kg [27], 0.184 kWh/kg [39]. This consistency further validates the adopted modelling approach and confirms that the simulated system operates within realistic thermodynamic limits.

An increase in ambient temperature also influences the unit energy gains during the expansion process, as illustrated in Figure 4. Higher inlet temperatures lead to increased air temperatures at the expander inlets after regasification, which enhances the specific expansion work. The relative changes in unit energy gains range from −5.3% at 0 °C to +7.12% at 35 °C with respect to the baseline case.

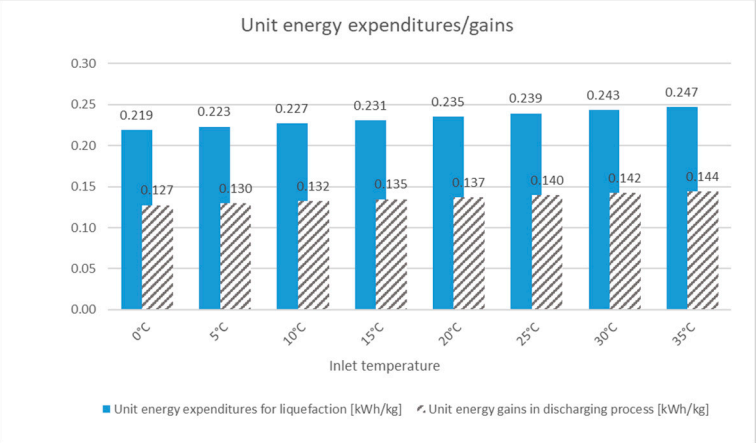


Figure 4. Unit energy expenditures/gains.

The slightly higher sensitivity of expansion energy gains, compared to liquefaction energy expenditures, may be attributed to differences in assumed turbomachinery efficiencies, as well as to the thermodynamic advantage of higher inlet temperatures during expansion. This effect partially compensates for the reduction in mass flow observed at elevated ambient temperatures.

The combined effects of temperature-dependent changes in liquefaction energy demand and expansion energy recovery result in a nearly constant round-trip efficiency, as shown in Figure 5. Across the investigated temperature range, the variation in efficiency remains within approximately 0.1%, which can be considered negligible from a practical standpoint.

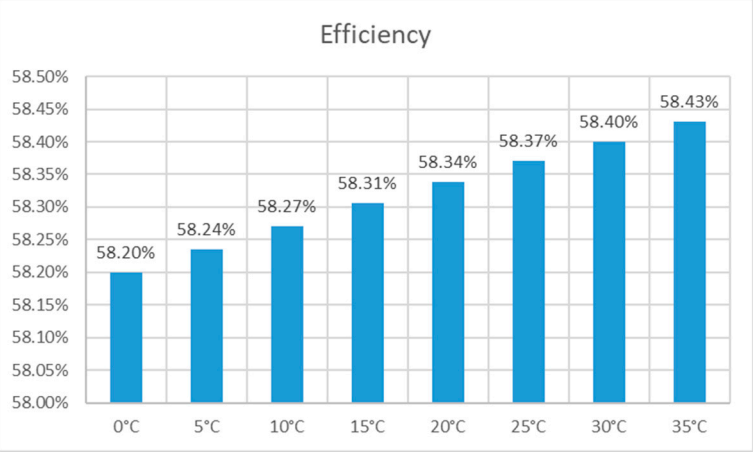


Figure 5. Round-trip efficiency for analyzed ambient temperatures.

This result demonstrates that ambient temperature has no significant impact on the overall efficiency of the LAES system, despite its influence on individual process parameters. Such robustness is a highly desirable feature for large-scale energy storage technologies, as it ensures stable performance under varying climatic conditions.

Although the round-trip efficiency remains almost unchanged, variations in inlet mass flow affect the absolute charging and discharging power levels. Figures 6 and 7 present the total charging and discharging power for the analyzed temperatures.

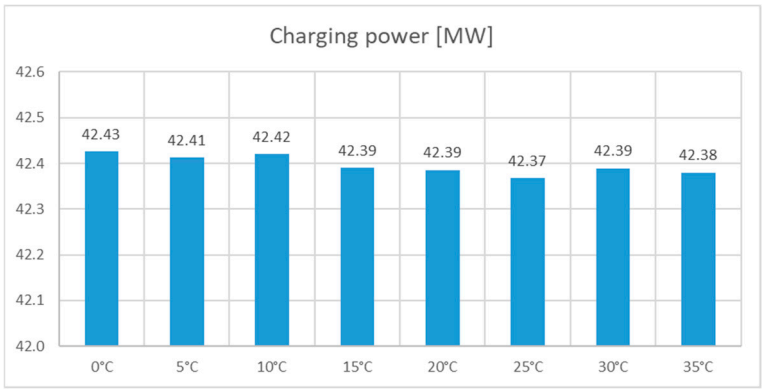


Figure 6. Charging power for analyzed ambient temperatures.

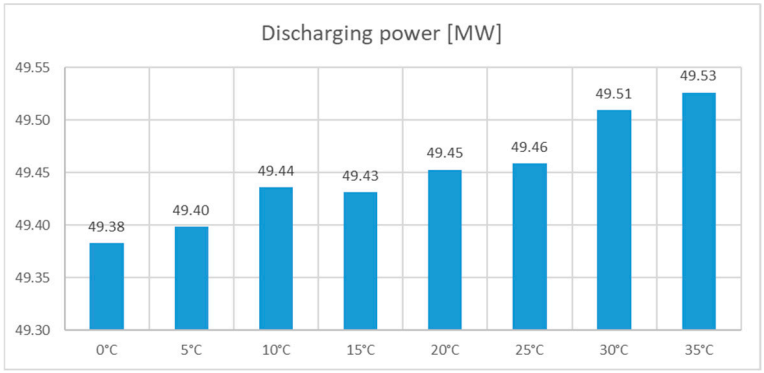


Figure 7. Discharging power for analyzed ambient temperatures, CDTR = 2.

As shown in Figure 6, the charging power slightly decreases with increasing ambient temperature, primarily due to the reduced inlet mass flow rate. The maximum observed difference between extreme cases (0 °C and 35 °C) is approximately 0.05 MW, which is negligible when compared to the nominal charging power of approximately 42.4 MW.

Conversely, the discharging power increases slightly with ambient temperature, as depicted in Figure 7 for a charging-to-discharging time ratio (CDTR) of 2. This trend can be explained by the higher thermal energy content of the working fluid at elevated temperatures, which outweighs the adverse effect of reduced mass flow on expander performance.

The results of this analysis indicate that LAES systems are largely insensitive to ambient temperature variations in terms of efficiency, while only marginal changes in charging and discharging power occur. This confirms that LAES technology can be effectively deployed across a wide range of climatic conditions without the need for significant performance derating or system redesign.

Consequently, the presented findings reinforce the technical viability and operational flexibility of LAES as a large-scale, long-duration energy storage solution, supporting its applicability in diverse geographic locations and energy system configurations.

5. Outcomes

The results of the simulations and thermodynamic analysis clearly demonstrate that ambient temperature exerts only a limited influence on the overall performance of the adiabatic LAES system. Across the investigated ambient temperature range of 0 °C to 35 °C, only minor variations were observed in key operational parameters, highlighting the system's high degree of thermal robustness under diverse climatic conditions.

Most notably, the round-trip efficiency of the installation remained practically constant, with values fluctuating around 58.3%. The observed deviations did not exceed ±0.1%,

indicating that adiabatic LAES systems can be effectively deployed in diverse geographic regions without significant efficiency losses. This result indicates that adiabatic LAES systems can be deployed across a wide range of geographic locations without experiencing meaningful efficiency degradation. Such stability reinforces the suitability of LAES technology for large-scale and long-duration energy storage in both temperate and warm climates. Changes in ambient temperature primarily affected the inlet mass flow rate of air. Compared to the baseline condition at 15 °C, the mass flow increased by approximately 5.5% at 0 °C and decreased by around 6.5% at 35 °C. This behavior can be attributed to the nature of volumetric compressors, which operate at a constant volumetric flow rate. Consequently, the mass of air processed depends directly on air density, which varies with temperature.

The specific energy consumption for the air liquefaction process also exhibited slight sensitivity to ambient temperature. Values ranged from 0.219 to 0.247 kWh/kg. These results remain fully consistent with values reported in the literature for high-pressure LAES configurations. A gradual increase in liquefaction energy demand was observed with rising ambient temperature, reflecting the higher compression work required at reduced air densities. In parallel, the specific energy recovered during the expansion process increased with temperature, displaying a slightly stronger temperature dependence. This asymmetry can be attributed to differences in the thermodynamic behavior and assumed efficiencies of compressors and expanders, as well as the beneficial effect of higher expander inlet temperatures on expansion work.

Although the round-trip efficiency remained stable, the total charging and discharging powers varied modestly due to the changes in mass flow. Charging power decreased slightly at higher ambient temperatures, resulting from lower air density, while discharging power increased slightly, benefiting from elevated temperatures at the expander inlets. These opposing effects effectively compensated for each other, further emphasizing the stable operational characteristics of the LAES system.

In conclusion, the analysis confirms that ambient temperature exerts only a marginal influence on the efficiency and performance of LAES systems. Therefore, such installations can be considered a technically viable and climate-resilient solution for large-scale energy storage, supporting the integration of intermittent renewable energy sources across various environmental conditions.

Author Contributions: Conceptualization, A.D. and P.K.; methodology, A.D. and P.K.; software, A.D.; validation, A.D.; investigation, A.D.; resources, A.D.; data curation, A.D.; writing—original draft preparation, A.D.; writing—review and editing, A.D. and P.K.; visualization, A.D.; supervision, P.K.; funding acquisition, A.D. All authors have read and agreed to the published version of the manuscript.

Funding: This research was partially funded by internal WUT funds in the form of the IDUB PW Young program, project title: Analysis of Liquid Air Energy Storage (LAES) system cooperation with variable-temperature cryogenic cold storage. no 504/04496/1131/45.180002.

Data Availability Statement: Data is contained within the article.

Conflicts of Interest: The authors declare no conflicts of interest.

Abbreviations

The following abbreviations are used in this manuscript:

LAES	Liquid Air Energy Storage
RES	Renewable Energy Sources
CDTR	Charging-to-Discharging Time Ratio
CAES	Compressed Air Energy Storage

Appendix A

Table A1. Main stream parameters for baseline case ($T_{ambient}$ = 15 °C).

Stream	Medium	Vapor Fraction	Temperature [°C]	Pressure [kPa]	Mass Flow [kg/s]
1	air	1	15.0	100.0	51.00
2	air	1	15.0	100.0	59.37
4	air	1	241.3	590.0	59.37
5	air	1	20.0	590.0	59.37
T5	n-C20	0	241.7	100.0	79.57
T5a	n-C20	0	241.7	100.0	79.57
T6a	n-C20	0	98.4	100.0	79.57
T6b	n-C20	0	15.0	100.0	79.57
T6c	n-C20	0	15.0	100.0	79.57
7	air	1	246.7	3400.0	59.37
8	air	1	20.0	3400.0	59.37
10	air	1	251.4	20,000.0	59.37
11	air	1	20.0	20,000.0	59.37
12	air	0	−179.0	20,000.0	59.37
13	air	0.142797	−188.0	200.0	59.37
14	air	1	−188.0	200.0	8.36
15	air	1	15.0	200.0	8.36
15a	air	1	15.0	200.0	8.37
16_17	air	0	−188.0	200.0	51.02
19	air	0	−182.7	10,000.0	51.02
20	air	1	−61.0	10,000.0	51.02
21	air	1	14.7	10,000.0	51.02
22	air	1	236.7	10,000.0	51.02
24	air	1	75.4	2154.4	51.02
25	air	1	236.7	2154.4	51.02
27	air	1	76.8	464.2	51.02
28	air	1	236.7	464.2	51.02
30	air	1	77.3	100.0	51.02
31_32	propane	0	−60.0	100.0	62.03
33_34	propane	0	−180.0	100.0	62.03
35_36	methanol	0	20.0	100.0	18.51
37_38	methanol	0	−60.0	100.0	18.51
38	n-C20	0	236.3	100.0	25.25
39	n-C20	0	241.7	100.0	25.82
40	n-C20	0	246.4	100.0	28.50
41	n-C20	0	241.7	100.0	26.26
42	n-C20	0	241.7	100.0	26.26
43	n-C20	0	241.7	100.0	27.05
44	n-C20	0	49.7	100.0	26.26
45	n-C20	0	117.4	100.0	26.26
46	n-C20	0	124.3	100.0	27.05
47	n-C20	0	15.0	100.0	25.25
48	n-C20	0	15.0	100.0	25.82
49	n-C20	0	15.0	100.0	28.50

References

1. Our World in Data. Global Primary Energy Consumption by Source. 2024. Available online: https://ourworldindata.org/grapher/global-energy-substitution (accessed on 23 October 2025).
2. Incer-Valverde, J.; Hamdy, S.; Morosuk, T.; Tsatsaronis, G. Improvement perspectives of cryogenics-based energy storage. *Renew. Energy* **2021**, *169*, 629–640. [CrossRef]
3. Ibrahim, H.; Ilinca, A.; Perron, J. Energy storage systems-Characteristics and comparisons. *Renew. Sustain. Energy Rev.* **2008**, *12*, 1221–1250. [CrossRef]
4. Arraño-Vargas, F.; Shen, Z.; Jiang, S.; Fletcher, J.; Konstantinou, G. Challenges and Mitigation Measures in Power Systems with High Share of Renewables—The Australian Experience. *Energies* **2022**, *15*, 429. [CrossRef]
5. Rahman, M.M.; Oni, A.O.; Gemechu, E.; Kumar, A. Assessment of energy storage technologies: A review. *Energy Convers. Manag.* **2020**, *223*, 113295. [CrossRef]
6. Dzido, A.; Wołowicz, M.; Krawczyk, P. Transcritical carbon dioxide cycle as a way to improve the efficiency of a Liquid Air Energy Storage system. *Renew. Energy* **2022**, *196*, 1385–1391. [CrossRef]
7. Deane, J.P.; Ó Gallachóir, B.P.; McKeogh, E.J. Techno-economic review of existing and new pumped hydro energy storage plant. *Renew. Sustain. Energy Rev.* **2010**, *14*, 1293–1302. [CrossRef]
8. Kantharaj, B.; Garvey, S.; Pimm, A. Compressed air energy storage with liquid air capacity extension. *Appl. Energy* **2015**, *157*, 152–164. [CrossRef]
9. Serrano-Arévalo, T.I.; Ochoa-Barragán, R.; Ramírez-Márquez, C.; El-Halwagi, M.; Jabbar, N.A.; Ponce-Ortega, J.M. Energy Storage: From Fundamental Principles to Industrial Applications. *Processes* **2025**, *13*, 1853. [CrossRef]
10. Borri, E.; Tafone, A.; Romagnoli, A.; Comodi, G. A review on liquid air energy storage: History, state of the art and recent developments. *Renew. Sustain. Energy Rev.* **2021**, *137*, 110572. [CrossRef]
11. Mongird, K.; Viswanathan, V.; Balducci1, P.; Alam, J.; Fotedar, V.; Hadjerioua, B.; Koritarov, V. Energy Storage Technology and Cost Report. 2019. Available online: https://www.osti.gov/servlets/purl/1573487 (accessed on 23 October 2025).
12. Guizzi, G.L.; Manno, M.; Tolomei, L.M.; Vitali, R.M. Thermodynamic analysis of a liquid air energy storage system. *Energy* **2015**, *93*, 1639–1647. [CrossRef]
13. Hamdy, S.; Moser, F.; Morosuk, T.; Tsatsaronis, G. Exergy-based and economic evaluation of liquefaction processes for cryogenics energy storage. *Energies* **2019**, *12*, 493. [CrossRef]
14. Damak, C.; Leducq, D.; Hoang, H.M.; Negro, D.; Delahaye, A. Liquid Air Energy Storage (LAES) as a large-scale storage technology for renewable energy integration—A review of investigation studies and near perspectives of LAES. *Int. J. Refrig.* **2020**, *110*, 208–218. [CrossRef]
15. O'Callaghan, O.; Donnellan, P. Liquid air energy storage systems: A review. *Renew. Sustain. Energy Rev.* **2021**, *146*, 111113. [CrossRef]
16. Olympios, A.V.; Mctigue, J.D.; Farres-Antunez, P.; Tafone, A. Progress and prospects of thermo-mechanical energy storage—A critical review Progress in Energy OPEN ACCESS Progress and prospects of thermo-mechanical energy storage—A critical review. *Prog. Energy* **2021**, *3*, 022001. [CrossRef]
17. Farres-Antunez, P.; Xue, H.; White, A.J. Thermodynamic analysis and optimisation of a combined liquid air and pumped thermal energy storage cycle. *J. Energy Storage* **2018**, *18*, 90–102. [CrossRef]
18. Georgiou, S.; Shah, N.; Markides, C.N. A thermo-economic analysis and comparison of pumped-thermal and liquid-air electricity storage systems. *Appl. Energy* **2018**, *226*, 1119–1133. [CrossRef]
19. Krawczyk, P.; Szabłowski, Ł.; Badyda, K.; Karellas, S.; Kakaras, E. Impact of selected parameters on performance of the Adiabatic Liquid Air Energy Storage system. *J. Power Technol.* **2016**, *4*, 238–244.
20. Howe, T.A.; Pollman, A.G.; Gannon, A.J. Operating Range for a Combined, Building-Scale Liquid Air Energy Storage and Expansion System: Energy and Exergy Analysis. *Entropy* **2018**, *20*, 770. [CrossRef] [PubMed]
21. Chen, A.; Nan, X.; Cai, X. Dynamic Modeling and Performance Analysis of Liquid Carbon Dioxide Energy Storage System. *Energies* **2025**, *18*, 2955. [CrossRef]
22. Peng, D.Y.; Robinson, D.B. A New Two-Constant Equation of State. *Ind. Eng. Chem. Fundam.* **1976**, *15*, 59–64. [CrossRef]
23. *HYSYS 2004.2 Simulation Basis, Aspen Tech Software Manual*; Aspen Technology, Inc.: Cambridge, MA, USA.
24. Liang, T.; Zhang, T.; Lin, X.; Alessio, T.; Legrand, M.; He, X.; Kildahl, H.; Lu, C.; Chen, H.; Romagnoli, A.; et al. Liquid air energy storage technology: A comprehensive review of research, development and deployment. *Prog. Energy* **2023**, *5*, 012002. [CrossRef]
25. Tafone, A.; Romagnoli, A. A novel liquid air energy storage system integrated with a cascaded latent heat cold thermal energy storage. *Energy* **2023**, *281*, 128203. [CrossRef]
26. An, B.; Chen, J.; Deng, Z.; Zhang, T.; Wang, J.; Yang, L.; Chang, X. Design and testing of a high performance liquid phase cold storage system for liquid air energy storage. *Energy Convers. Manag.* **2020**, *226*, 113520. [CrossRef]
27. Dzido, A.; Krawczyk, P.; Wołowicz, M.; Badyda, K. Comparison of advanced air liquefaction systems in Liquid Air Energy Storage applications. *Renew. Energy* **2022**, *184*, 727–739. [CrossRef]

28. Mehrpooya, M.; Mehdi, M.; Sharifzadeh, M.; Rosen, M.A. Optimum design and exergy analysis of a novel cryogenic air separation process with LNG (liquefied natural gas) cold energy utilization. *Energy* **2015**, *90*, 2047–2069. [CrossRef]
29. Mikołajczak, A.; Wołowicz, M.; Kurkus-Gruszecka, M.; Badyda, K.; Krawczyk, P. Improving the efficiency of Liquid Air Energy Storage by organic rankine cycle module application. In *2018 International Interdisciplinary PhD Workshop (IIPhDW)*; Curran Associates, Inc.: Red Hook, NY, USA, 2018; pp. 99–102. [CrossRef]
30. Bhavsar, S.; De, S. Aerodynamic design and performance evaluation of pipe diffuser for centrifugal compressor of micro gas turbine. In Proceedings of the ASME 2019 Gas Tirbine India, Chennai, India, 5–6 December 2019.
31. Li, P.; Zuo, Z.; Zhou, X.; Li, J.; Chen, H. Investigation of Different Rotational Speed Characteristics of Multistage Axial Compressor in CAES System. *Energies* **2023**, *16*, 4383. [CrossRef]
32. Shahri, M.H.; Madadi, A.; Boroomand, M. Three—Dimensional Optimization of Blade Lean and Sweep for an Axial Compressor to Improve the Engine Performance. *J. Appl. Fluid Mech.* **2023**, *16*, 2206–2218.
33. Kumar, A.; Singh, A. Numerical Optimization of a Radial Inflow Turbine Based on a Loss Model of a Cryogenic Turboexpander Using the Slime Mould Algorithm. *Def. Sci. J.* **2025**, *75*, 512–519. [CrossRef]
34. Li, H.; Li, W.; Zhang, X.; Zhu, Y.; Zuo, Z.; Qin, W.; Chen, H. Characteristic of a multistage reheating radial inflow in supercritical compressed air energy storage with variable operating parameters. *Proc. Inst. Mech. Eng. Part A J. Power Energy* **2018**, *233*, 397–412. [CrossRef]
35. She, X.; Peng, X.; Nie, B.; Leng, G.; Zhang, X.; Weng, L.; Tong, L.; Zheng, L.; Wang, L.; Ding, Y. Enhancement of round trip efficiency of liquid air energy storage through effective utilization of heat of compression. *Appl. Energy* **2017**, *206*, 1632–1642. [CrossRef]
36. Sciacovelli, A.; Vecchi, A.; Ding, Y. Liquid air energy storage (LAES) with packed bed cold thermal storage—From component to system level performance through dynamic modelling. *Appl. Energy* **2017**, *190*, 84–98. [CrossRef]
37. Hüttermann, L.; Span, R.; Maas, P.; Scherer, V. Investigation of a liquid air energy storage (LAES) system with different cryogenic heat storage devices. *Energy Procedia* **2019**, *158*, 4410–4415. [CrossRef]
38. Szablowski, L.; Krawczyk, P.; Wolowicz, M. Exergy analysis of adiabatic liquid air energy storage (A-laes) system based on linde–hampson cycle. *Energies* **2021**, *14*, 945. [CrossRef]
39. Krawczyk, P.; Szabłowski, Ł.; Karellas, S.; Kakaras, E. Comparative energy and exergy analysis of compressed air and liquid air energy storage systems. In Proceedings of the 29th International Conference on Efficiency, Cost, Optimisation, Simulation and Environmental Impact of Energy Systems ECOS 2016, Portorož, Slovenia, 19–23 June 2016.

Disclaimer/Publisher's Note: The statements, opinions and data contained in all publications are solely those of the individual author(s) and contributor(s) and not of MDPI and/or the editor(s). MDPI and/or the editor(s) disclaim responsibility for any injury to people or property resulting from any ideas, methods, instructions or products referred to in the content.